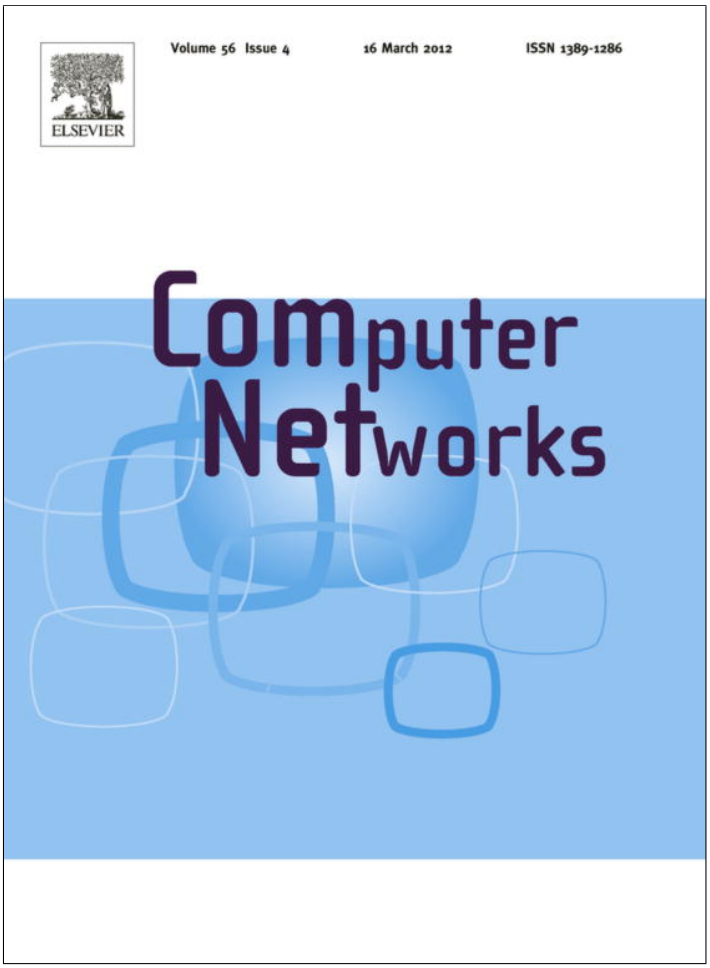

Computer Networks 56 (2012) 1236–1248

Contents lists available at SciVerse ScienceDirect

Computer Networks

journal homepage: www.elsevier.com/locate/comnet

Contention based scheduling for femtocell access points in a densely deployed network environment

Jeongkyun Yun [a], Sung-Guk Yoon [b,*], Jin-Ghoo Choi [c], Saewoong Bahk [b]

[a] LG Electronics, Seoul, Republic of Korea
[b] INMC, School of EECS, Seoul National University, Seoul, Republic of Korea
[c] Department of Information and Communication Engineering, Yeungnam University, Gyeongsangbuk-do, Republic of Korea

ARTICLE INFO

Article history:
Received 8 August 2011
Received in revised form 2 December 2011
Accepted 3 December 2011
Available online 10 December 2011

Keywords:
Self organizing network
Femtocell
Contention scheduling

ABSTRACT

The proliferation of new data intensive devices has caused an enormous burden on wireless systems. A femtocell network is a promising new technology developed to meet these demands. Since each femtocell network consists of uncoordinated subnetworks that work independently, the interference between subnetworks can result in a significant degradation of the overall network capacity. In this paper, we address the interference problem between uncoordinated femtocell access points (FAPs) and propose a distributed FAP scheduling scheme in a densely deployed femtocell network where FAPs interfere with each other. In contrast to previous works that have focused on dynamic power and frequency management, our approach focuses on time sharing through FAP contention. Depending on the outcome of contention, our method selects a winning FAP to be the sole user of the next time frame. The approach operates in a fully distributed manner with help from mobile nodes (MNs). To implement this scheme, we develop a new synchronous frame structure, which uses special common control channels. Through simulations, we observe that the proposed scheme doubles the network capacity compared to the legacy non-contending scheme, and could serve as the basis for future standards on femtocell networks.

1. Introduction

While wireless communications originated from very humble beginnings at a few bits per second, by exchanging Morse codes, upcoming fourth generation wireless technologies (for instance, IEEE 802.11n, 802.16m and LTE-advanced) are expected to achieve wireless capacities of up to 1 Gbps. According to the Cooper's Law, the wireless capacity has doubled every 30 months over the last 100 years [1]. The main factor of the increase in capacity has been the reduction in cell size, which contributed to an increase of 1,600 times, while advanced physical (PHY) and media access control (MAC) layer technologies, such as modulation and resource management schemes, have contributed to only an increase of 25 times in performance [1].

The important advantage of reducing the cell size is that the receiver is able to receive data packets at a high signal to noise ratio (SNR). Conventional wireless networks take advantage of this smaller cell size in increasing the wireless capacity since receivers can get the desired signal with higher strength. However, the gain obtained from the smaller cell size could get compromised by the heavy interference caused by the close proximity of neighboring cells. This means that network systems are increasingly becoming interference limited. Thus, a more important metric for network capacity is the signal to interference-plus-noise ratio (SINR) rather than SNR [2]. Therefore, each transmitter in a cell should not use its maximum power to transmit in order to reduce interference to neighboring

* Corresponding author. Tel.: +82 28808434; fax: +82 28808198.
E-mail addresses: jyun@netlab.snu.ac.kr (J. Yun), sgyoon@netlab.snu.ac.kr (S.-G. Yoon), jchoi@yu.ac.kr (J.-G. Choi), sbahk@snu.ac.kr (S. Bahk).

1389-1286/$ - see front matter © 2011 Elsevier B.V. All rights reserved.
doi:10.1016/j.comnet.2011.12.003

cells. That is, simply reducing the cell size is no longer effective in increasing the network capacity in this interference limited paradigm. These days interference mitigation has become a highly challenging issue because most of the advanced wireless technologies adopt a frequency reuse factor (FRF) of one to maximize system spectral efficiency.

The latest technology in reducing the cell size is to use femtocells [3] that can be created by individual subscribers. In a femtocell network, a femtocell access point (FAP) takes charge in functioning as a macro base station (BS) to cover a small area. Since both femtocell networks and wireless local area networks (WLANs) have similar features in many things, we can easily anticipate that problems in femtocell networks will be similar with the current problems in WLANs. Due to densely deployed WLAN access points (APs), the most severe problem in WLANs is the interference between APs. This is because subscribers can install APs for themselves without consideration of other existing APs, and this problem is the same to femtocell networks. For instance, Fig. 1 shows a qualitative measurement of WLAN channel occupancy rate. We measured the channel occupation rate in a common apartment building in Korea, using a WLAN AP of Anygate RG-3000A [4]. The graph says that our AP could hear 16 APs, which implies 16 interferers co-exist in this residential area. In conclusion, to maximize the femtocell gain, femtocells should solve the interference mitigation problem as well [2,5].

However, the interference mitigation in femtocell is harder to implement than that in conventional macrocell for several reasons [3]: First, FAPs normally use the Internet as the backbone network, so there is no explicit interface between FAPs. Second, FAPs are characterized by poorer computing power than macro BSs due to the cost down. Lastly, individual subscribers are expected to set up FAPs in an uncoordinated manner. Therefore, the interference mitigation algorithm for the femtocell network should be simple and distributed.

1.1. Related work

Combating interference is a key issue in designing a femtocell network [2,5,6]. There are two types of interference problems in the femtocell network: One is the interference between macrocell and femtocell, and the other between femtocells themselves. Regarding the first problem, if macrocell and femtocell networks operate in the same frequency band and try to mitigate the interference, some specification changes need to be made since femtocells are deployed in an uncoordinated manner [2]. There have been certain approaches proposed to solve this problem by controlling transmission power or by allocating different frequency bands to the macrocell and femtocells, respectively. Power control based interference mitigation schemes [7–9] tried to make the most interfered users, located between the macro BS and an FAP, have at least the same received power. In the frequency allocation based interference mitigation schemes [10,11], the FAP operates in a different frequency band from the macro BS, resulting in higher SINR but lower spatial reuse.

For the second interference problem, power control based solutions work the same as to the first problem. They try to control FAP's transmission power such that the strength of the desired signal at least equals that of interference signal. Many frequency based solutions have been proposed. Li et al. [12] have proposed a fractional frequency allocation scheme for FAPs through sensing each other's interference level. However, their solutions rely on a strong assumption that each FAP fully understands the interference condition. In [13], they have proposed a distributed random access scheme that uses a hashing function to avoid interference between femtocells.

However, in a densely deployed network, the interference cannot be sufficiently mitigated by only frequency planning or power control. The research in [14] shows that deactivating some users leads to better performance than activating all the users simultaneously. To this end, a

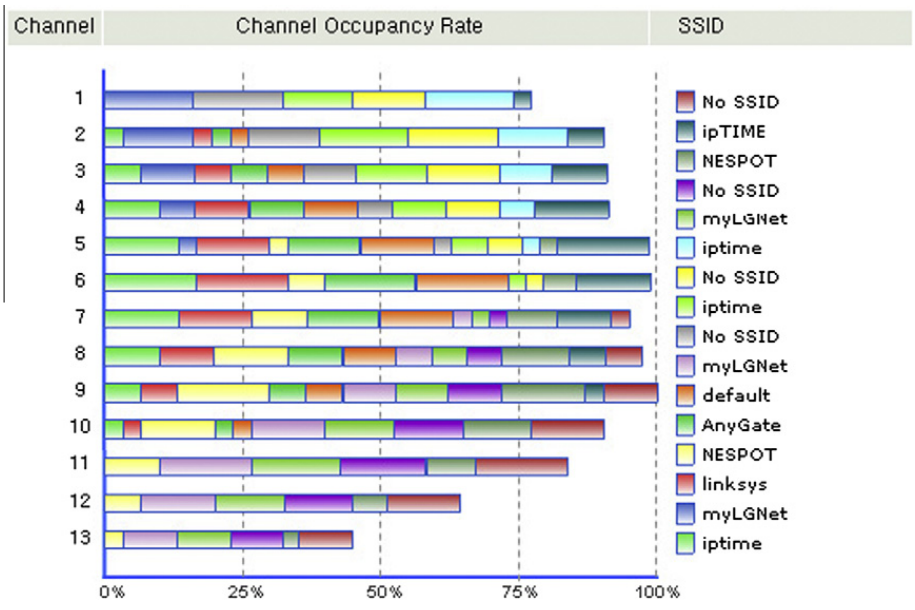

Fig. 1. Channel occupancy rate of WLAN APs in an apartment building.

technical report [15] from 3GPP has proposed an interference reduction scheme that allocates different frame access patterns to each FAP and the macro BS, respectively, in time domain but each pattern should be allocated by a centralized controller. Another 3GPP document in [16] has considered a centralized interference mitigation approach between macrocell and femtocell. It makes the macro BS use 'almost blank subframes' which allow femtocells to transmit without suffering from the macrocell interference.

Rather than a centralized approach, distributed femtocell interference mitigation schemes for a densely deployed network have been recently investigated. Garcia et al. [17] has proposed a frequency allocation scheme that exploits different subchannels in a carrier aggregated frequency band. Another research [18] has formulated a coalition game for femtocell interference management. In [14], the authors have proposed a new framework to measure the interference level and a dynamic frequency allocation algorithm. However, all the investigations assumed a management entity in the backbone network to gather interference information and to make a decision in allocating time and frequency resources, or assumed interference information exchanges between FAPs through the backbone network.

Our proposed algorithm does not require any coordination between the backbone and femto networks. We aim to reduce femto-to-femto interference by time scheduling in a distributed manner. It exploits FAP contention positively, without requiring any help from the macro BS or other FAPs. It also tries to activate as many APs as possible if femtocell networks can permit. Each FAP contends with each other to get a right to use the channel. To implement our algorithm in a fully distributed manner, mobile nodes report the FAP contention result to the associated FAPs through a common control channel specified in our proposed frame structure.

This paper is organized as follows. Section 2 presents our proposed frame structure and FAP contention based scheduling algorithm. We examine the performance of our proposed scheme through analysis and simulation in Sections 3 and 4, respectively. The concluding remarks follow in Section 5.

2. Proposed channel access method

For clarity of exposition, we assume that all FAPs in the interference dominant network use only a single frequency band. In addition, we assume that the network use a time-division duplex (TDD) based orthogonal frequency division multiple access (OFDMA) system, and that frames among FAPs are synchronized. However, our proposed scheme can easily adopt other multiple access and duplex schemes such as a frequency-division duplex (FDD) based OFDMA or code division multiple access (CDMA) system.

Our target is to activate only one FAP among FAPs within a given interference domain[1] in a distributed manner. For example, in Fig. 2, FAPs 1 and 2 try to send data to MNs 1 and 2, respectively. In the legacy scheme, the FAPs should use a low modulation and coding scheme (MCS) to overcome the interference from each other. Another way to reduce the interference is for each FAP to transmit data in turn, i.e. FAPs 1 and 2 use different time frames.

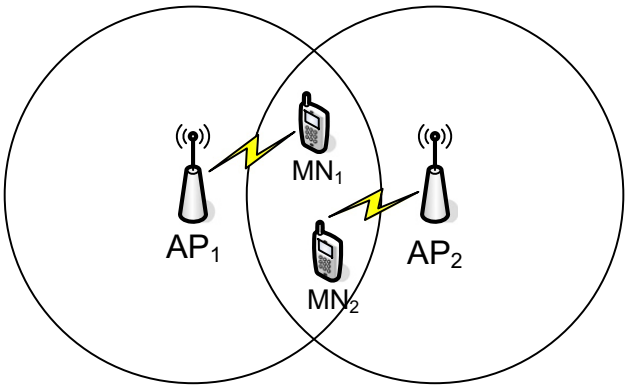

Fig. 2. Example of the interference.

Before explaining our proposed scheme, we briefly illustrate the impact of a time scheduling algorithm on network capacity. In Fig. 2, the two FAPs simultaneously use the entire time frame under low SINR when the legacy scheme is applied. In contrast, they are allowed to use half the time frame each under high SINR if a time scheduling scheme is applied. From the Shannon capacity formula, which is given as $\log_2(1 + SINR)$, we obtain the capacity of each scheme for an FAP as

$$C = \begin{cases} \log_2(1 + \mathrm{SINR}_{int}) & \text{for legacy scheme,} \\ \frac{1}{2}\log_2(1 + \mathrm{SINR}_{clr}) & \text{for time scheduling scheme,} \end{cases} \quad (1)$$

where $SINR_{int}$ and $SINR_{clr}$ represent the SINRs with and without interference, respectively. Because the two FAPs share time resource, the capacity of each FAP has been reduced by half. In a high interference area, the $SINR_{int}$ could be almost equal to 1, so the capacity is 1 b/s/Hz. If $SINR_{clr}$ is larger than 3, which is 4.8 dB, the network capacity with the time division FAP scheduling scheme is larger than without it. For a densely deployed network, in general, $SINR_{clr}$ is three times larger than $SINR_{int}$ since each MN is usually associated with an in-home installed FAP. Therefore, we expect that the FAP time scheduling scheme should outperform the legacy scheme.

2.1. Contention enabling frame structure

To handle the interference problem in a distributed manner, we first consider a contention enabling synchronous frame structure. Fig. 3 depicts an example of our proposed structure. This is a simple modification of a traditional TDD and OFDMA based cellular frame structure proposed by WiMAX [19]. The only difference from the legacy structure is that it additionally uses one FAP engaging channel (AEC) and two FAP indicator channels (AICs) for downlink and uplink, respectively.

AEC and AIC use a small number of OFDMA symbols. In this example, each of AEC and AIC uses one resource block

[1] We define the interference domain in Section 2.2.

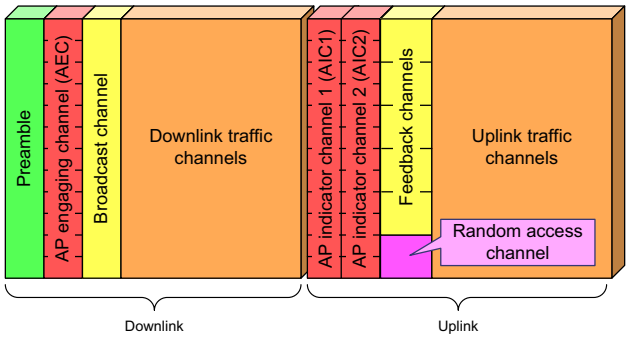

Fig. 3. Contention enabling synchronous frame structure for TDD OFDMA system.

Table 1
AIC information.

AIC1	AIC2	Meaning
0	0	Win the contention, and use the next frame
1	0	Lose the contention, and do not use the next frame
0	1	Collision, and reselect AEC/AICs pair
1	1	Reserved

which consists of one symbol time and several sub-channels. Every AEC has corresponding AICs (AIC1 and AIC2). During the initialization procedure, each FAP should obtain its own AEC/AICs pair which do not overlap with those of neighboring FAPs. Each FAP transmits a random number for contention through its own AEC. AICs carry binary information only, so one bit of information is enough for each AIC, i.e. the OFDM symbol of busy or idle. We represent at least one busy signal as '1' and no busy signal as '0.' Because of the use of one bit signaling, there is no collision in AIC. That is, when a collision occurs, it is understood as '1.' AIC1 and AIC2 send the result of the contention and collision, respectively. The values '0' and '1' received from AIC1 mean that the FAP which sent a random number through the corresponding AEC won and lost the contention, respectively. Similarly, '0' from AIC2 indicates that AEC data received without collision and '1' indicates collision. The meanings of the two bits in the AICs are listed in Table 1.

2.2. Notations

We now define some notation to explain the detailed algorithm for our proposed scheme.

- A_i: Access point i.
- M_{ij}: Mobile node j associated with A_i.
- $C(A_i)$: The set of MNs that receives signals with sufficiently high SINR from A_i.
- $C(M_{ij}) = \{A_k | M_{ij} \in C(A_k), \forall k\}$. That is, the set of all A_k which holds that M_{ij} belongs to A_k's defined coverage.
- $NB(A_i)$: The set of neighbor FAPs that share at least one MN with A_i, i.e. the interference domain of A_i.
- S_f: Current frame sequence number.
- N_{ch}: Total number of AEC/AICs pairs.
- c_i: AEC/AICs pair number obtained by A_i.
- W: Contention window size.
- r_i: Random number used by A_i during contention.
- P_i: Activation probability of A_i at a given frame.
- U: Channel utilization.

2.3. Contention for channel access

Our aim is to enable an FAP A_i to use the shared medium exclusively. That is, A_i should be the only active FAP among $A_i \cup NB(A_i)$ at a specific time frame. We use the same channel access method for both downlink and uplink transmissions. To access the channel, each FAP first contends with neighboring FAPs. When an FAP wins the channel contention, it can use the next time frame exclusively and schedule data transmissions for MNs in its own domain. The definition of a 'neighbor FAP' is not one-hop connected FAPs but the FAPs who share at least one MN in their shared coverage, as shown in Fig. 4(b). Therefore, in Fig. 4(a), the FAPs are not neighbors of each other unless an MN appears in the shared area.[2]

The contention method works as follows. In the first frame, each FAP A_i selects a random number r_i within the contention window $[0, W)$, and broadcasts r_i through its own AEC c_i. Each MN M_{ij} hears all the random numbers broadcasted by their neighbor FAPs $C(M_{ij})$, and decides a winner, i.e. the smallest r_i. When a winner is decided, every MN who hears AEC replies via each corresponding AIC1 of all the losing FAPs. Since these AIC responses do not have any information besides signaling, i.e. busy or idle, there is no collision problem in the AIC response.

When an FAP wins the contention, it is eligible to exclusively use the next time frame as depicted in Fig. 5. This figure illustrates the contention procedure as follows. When an FAP A_i wants to access the wireless medium, it first transmits a random number r_i over its own AEC c_i. After hearing this signal, the MNs transmit the result of the contention through the corresponding AIC1 only to the losers (not the winner). This means that the FAP which receives no response wins the contention. The winning FAP uses the next frame (both downlink and uplink) for its own traffic and lost FAPs should not transmit and schedule uplink data at all.[3]

There are two types of collision: One is a random number collision which occurs when more than one FAP chooses the same smallest number, and the other is AEC collision which occurs when more than one FAP chooses the same AEC/AICs pair. For the random number collision, the corresponding MNs break the tie as follows. According to the current frame sequence number S_f, if S_f is odd (or even), they select an FAP that uses the AEC with the lowest (or highest) c_i as the winner.

For the AEC collision problem, the corresponding MNs in the shared area recognize the collision, and are respon-

[2] We assume that all FAPs are synchronized as in cellular networks.

[3] If there are more than two FAPs who have received no response due to some reason such as channel error, they will transmit in the next frame time and collision occurs. They will repeat the same process until the collision is resolved. However such collision does not always mean transmission failure. Owing to the capture effect, the transmission can be made successful in many cases.

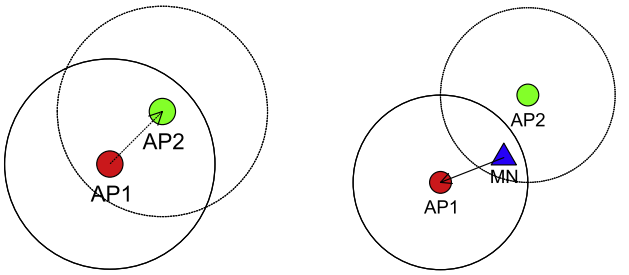

(a) Although the two FAPs can see each other but share no MN, they are not 'neighbor FAPs.'

(b) Since the two FAPs share a common MN, they are 'neighbor FAPs.'

Fig. 4. Definition of 'neighbor FAPs'

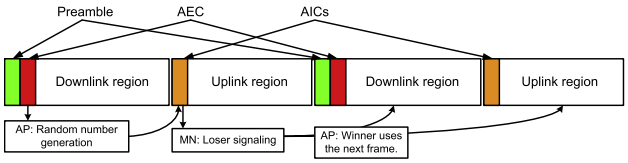

Fig. 5. Frame allocation using AEC/AICs pair contention.

sible for reporting it to the FAPs involved. To resolve this collision, these FAPs must select another AEC/AICs pair randomly until the selected channel pair is clear. The detailed collision resolution mechanism is described in the next subsection.

2.4. Procedures for AEC/AICs pair allocation

Each FAP should have its own non-overlapping AEC/AICs pair to contend with other FAPs. To obtain an AEC/AICs pair, a newly joining FAP A_i listens to all the AECs for some time to build the table of busy AEC/AICs pairs. Then, A_i randomly selects one idle AEC/AICs pair among the idle ones, and uses it for contention. An AEC collision may occur if a neighbor FAP chooses the same AEC/AICs pair by chance, or a new MN appears in the shared area while two FAPs are using the same AEC/AICs pair.

For example, in the case of Fig. 4(a), if the two FAPs share no MNs, they can use the same AEC/AICs pair without experiencing AEC collision, but in the case of Fig. 4(b), the two FAPs need to use different AEC/AICs pair. If the two FAPs use the same AEC, M_{ij} can hear neither of the two FAPs. M_{ij} informs this AEC collision to the FAPs by transmitting a '1' through the corresponding AIC2. All FAPs using this AEC hear the message to recognize whether they were involved in a collision or not. If the FAP is informed of an AEC collision, it randomly selects another AEC/AICs pair among the idle channel pairs.

2.5. Overhead for using AEC/AICs pair

In our FAP contention scheme, the system must use two special common control channels (AEC and AIC), which convey the contention information. Since these additional channels can be viewed as overhead, we now calculate the size of the overhead when the Mobile WiMAX specification [19] is applied.

For the downlink case, there are 720 data sub-carriers out of 1024 total sub-carriers per OFDMA symbol.[4] The data sub-carriers are divided into 30 sub-channels, and one sub-channel corresponds to the downlink resource allocation unit. That is, each sub-channel has 24 sub-carriers per symbol. We assume that one AEC consumes one sub-channel in one symbol. For FAP contention, the AEC information must successfully reach all MNs within the transmission range of each FAP. The frame control header (FCH[5]) is also very important, and it uses not only low modulation (QPSK) and coding rate (1/2) but also four repetition codes to protect the information. Assuming that the AEC information also uses the same repetition, modulation, and coding with FCH; one AEC can carry six bits.[6] Note that this is conservative usage since an FAP's transmission range is much smaller than that of macro BS, and the femtocell environment is normally indoor. Through the six bits, each FAP can select a random number in [0,64) for contention; it is large enough to keep the probability of random number collision between FAPs very small.

The resource unit of the uplink is a tile which consists of three OFDMA symbol and four sub-carriers. To ensure that the AIC is robust enough, we use three tiles which are the same number of tiles on one ACK transmission. Note that using three tiles for one AIC is also conservative usage because of the same reason as in the downlink case.

We now can calculate the additional overhead of the AEC/AICs pairs under the above two assumptions. Excluding the original overhead,[7] a frame of Mobile WiMAX normally has 26 OFDMA symbols for downlink and 840 tiles for uplink. There are two AICs corresponding to one AEC, which are AIC1 and AIC2. Assuming that n AEC/AICs pairs are added using our proposed frame structure, the portions of the additional overhead are $\frac{24n}{26\times720}$ and $\frac{6n}{840}$ for downlink and uplink, respectively. In the case of 20 AEC/AICs pairs, the additional overhead is 2.56% and 14.3% for downlink and uplink, respectively. Despite the overhead, the simulation results in Section 4 show that our proposed scheme outperforms the conventional scheme.

2.6. Operation example

This section explains our proposed scheme through an example shown in Fig. 6. There are three FAPs and four MNs involved within the network, and each A_i has one or two serving MNs (M_{ij}) in its service region. We set $N_{ch} = 10$ and $W = 16$. The entire scenario is presented in Table 2.

Initial state: M_{11} is located out of the shared area. That is, A_1 and A_2 do not interfere with each other even though A_2 is in the range of A_1 and vise versa. However, when M_{11} moves to M^*_{11}, A_1 and A_2 become interfering neighbors.

At frame 1: When the scenario starts, each FAP randomly chooses one AEC/AICs pair out of N_{ch}. Let the FAPs

[4] We assume that the system uses 10 MHz bandwidth and OFDMA/TDD.

[5] FCH is header for the MAP message.

[6] Through four repetition, 1/2-convolution coding, and QPSK modulation; to carry six bits, it needs 24 sub-carriers ($4 \times 2 \times 1/2 \times 6 = 24$).

[7] Downlink control channels: FCH, DL-MAP, UL-MAP; uplink control channels: CQICH, ACK, Ranging channel.

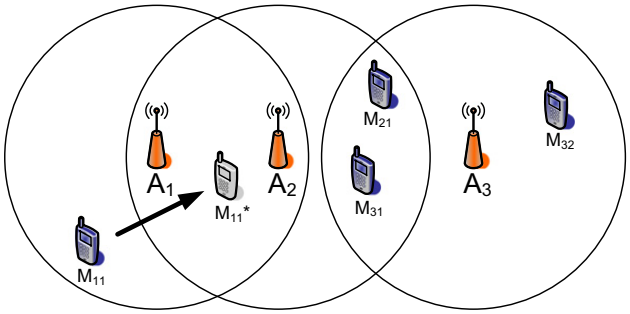

Fig. 6. Example topology.

Table 2
Contention example.

FAP id	AEC		AIC1 (win/lose)	AIC2 (collision)
	Sub-channel#	Random#		
First frame				
1	4	12		
2	4	6		
3	5	10	M_{21}, M_{31}	
* Event: M_{11} moves to $M_{11}^{*} \rightarrow A_1$ and A_2 become neighbors.				
Second frame				
✓1	4	1		M_{11}
✓2	4	11	M_{21}, M_{31}	M_{11}
3	3	7		
Third frame				
1	5	3		
2	7	4	M_{11}, M_{21}, M_{31}	
✓3	3	4		
Fourth frame				
✓1	5	1		
2	7	2	M_{11}	
✓3	3	4	M_{21}, M_{31}	
Fifth frame				
✓1	5	5		
2	7	10	M_{11}, M_{21}, M_{31}	
3	3	8		

A_1 through A_3 randomly pick the AEC/AICs pair c_i of 4, 4, and 5, respectively. Each FAP i also picks a random contention number r_i in contention window $[0,W)$. Let the selected r_i's be 12, 6, and 10, respectively at the first frame, and each FAP i transmits r_i via its own AEC c_i. Since A_1 and A_2 currently share no MN, they do not suffer from AEC collision. In addition, A_1 and A_2 do not need to contend, so A_1 and A_2 can simultaneously serve their MNs, i.e. M_{11} and M_{21}, without suffering from interference. However, since two MNs (M_{21} and M_{31}) are in the shared area of A_2 and A_3, A_2's communication interferes with the communication between A_3 and M_{31}. Therefore, A_2 and A_3 should contend for the frame to avoid simultaneous activation. Fortunately, A_2 and A_3 select different AEC/AICs pairs, so M_{21} and M_{31} can decode their random numbers r_2 and r_3 broadcast via c_2 and c_3, respectively. Because A_3 chooses a larger number compared to A_2, M_{21} and M_{31} inform A_3 that they have lost the contention. As a result, in the second frame, A_1 and A_2 are activated. In Table 2, we check the active FAPs with check marks (✓) beside each FAP id. At the end of the first frame, M_{11} moves to M_{11}^{*}, so that A_1 and A_2 become neighbors of each other.

At frame 2: Because A_1 and A_2 collide with each other in AEC 4 in the second frame, M_{11} cannot decode the received random numbers r_1 and r_2 transmitted by A_1 and A_2, respectively. M_{11} informs the FAPs of this AEC collision via the AIC2. After receiving this message, A_1 and A_2 randomly choose another AEC/AICs pair again among the idle channel pairs. A_3 wins the contention, so A_3 can use the next frame.

At frame 3: In this frame, A_1 and A_2 choose different AECs, i.e. $c_1 = 5$ and $c_2 = 7$, because of the AEC collision in the second frame. Therefore, there is no AEC collision from the third frame, that is, each A_i can contend with its neighbors $NB(A_i)$. In this frame, A_1 and A_3 win the contention. M_{11}, M_{21}, and M_{31} inform A_2 that they have lost the contention through the AIC1. Note that A_2 and A_3 break the tie using the tie-breaking rule, that is, the lowest channel numbered FAP wins at an odd frame sequence number. The active FAPs in the fourth frame are A_1 and A_3.

At frame 4: The fourth frame shows a worst case scenario. A_2 and A_3 are beaten by their neighbor FAPs. Only A_1 is activated for the fifth frame. To overcome this inefficiency, we next propose an extension called multi-frame contention.

2.7. Multi-frame contention

To further improve channel utilization, we propose a multi-frame contention mechanism that uses the multi round contention to select multiple FAPs eligible to use next multiple frames, which results in a greater number of activated FAPs.

We combine R frames into one super frame which consists of R-rounds of the contention mechanism.[8] After going through an R-round contention, the winning multiple FAPs can exclusively use the next super frame of R frames. Each winner FAP i uses '-1' as the r_i for next contention throughout the same super frame to keep itself as the winner by the end of the super frame. The lost FAPs get more chances to win during the same super frame.

For instance, in the fourth frame case discussed in the previous example, we assume that the fourth and fifth frames are for one super frame ($R = 2$). Since A_1 won the previous frame, it sets $r_1 = -1$ in the fifth frame while the other FAPs choose random numbers as shown in Table 2. As a result, A_1 and A_3 can be activated during the sixth and seventh frames that are the next super frames. Following this way, the multi-frame contention mechanism can improve the channel utilization.

3. Performance analysis

In this section, we analyze the channel utilization when using our proposed FAP contention based scheduling scheme for a simple chain topology. We define the channel utilization U as the ratio of the number of active FAPs to the total number of FAPs in the network.

[8] Each frame indicates a round.

3.1. Chain topology without multi-frame contention

We consider a simply connected chain topology as shown in Fig. 7, where the chain length[9] is K. Here, 'connected' means that every FAP must contend with its nearby FAPs. That is, neighboring FAPs share at least one MN. Let tr and d be the transmission range of an FAP and the distance between two neighboring FAPs, respectively. For the considered topology, we obtain the following Lemma 1.

Lemma 1. *In the simply connected chain topology with $tr < d \leqslant 2tr$, the channel utilization is given by*

$$U = \begin{cases} 1, & \text{when } K = 1, \\ \frac{K+1}{3K} - \frac{K-2}{12KW^2}, & \text{when } K \geqslant 2. \end{cases} \quad (2)$$

The proof is presented in the Appendix A. When K is larger than one, the second term in (2) can be ignored if W is large enough. For instance, if $W = 64$ and $K = 20$ which is similar with our simulation environment, we can ignore the second term. Therefore, we approximate the utilization U as follows

$$U \approx \frac{K+1}{3K}. \quad (3)$$

3.2. Multi-frame contention effect

In this subsection, we analyze the effect of multi-frame contention on channel utilization in the connected chain topology. For simplicity, we assume an infinite contention window W, that is, each FAP i can choose a unique r_i for each frame. This is a reasonable assumption since the tie breaking rule in our scheme works in a nearly random manner.

3.2.1. Definition of inactive chain type

The inactive chain is a chain that consists of consecutive inactive FAPs. Its edges may be vacant or active FAPs. We can define three types of chains based on the edge condition: initial type (I-type), edge type (E-type), and middle type (M-type). In the I-type chain, both edges of the chain are vacant as depicted in Fig. 8(a). Only a chain without active FAPs can be I-type. The E-type chain has one vacant edge and one active FAP edge as shown in Fig. 8(b). Only I-type and E-type chains can generate an E-type chain at the next round contention. Lastly, the M-type chain has active FAPs at both ends as shown in Fig. 8(c). This can be generated from any type of the chain of the previous round.

3.2.2. Activation probability of an inactive FAP

We define $A_I(p)$, $A_E(p)$, and $A_M(p)$ as functions that return the probability of an inactive FAP turning into active after one contention round for each chain type I, E, and M, respectively, when the chain length is p.

In the I-type chain, the multi-round contention is the same as the single round contention case, so we can get $A_I(p)$ from Lemma 1. According to (2) for a large W, we have

[9] The number of FAPs in the connected chain.

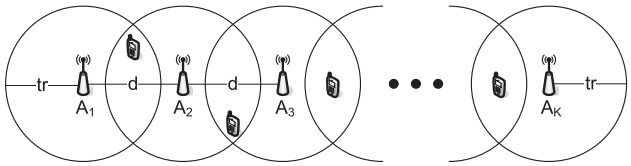

Fig. 7. Simple chain topology with K FAPs. tr and d denote the transmission range of FAP and the distance between two neighboring FAPs.

$$A_I(p) = \begin{cases} 1 & \text{for } p = 1, \\ \frac{p+1}{3p} & \text{for } p \geqslant 2. \end{cases} \quad (4)$$

In the E-type chain, $A_E(p)$ is the same as $A_I(p)$ except that one of the edge FAPs neighboring to an active FAP has zero probability of activation. As shown in the Appendix A, the expected value of activation probability of the edge FAP is 1/2. Therefore, we have

$$A_E(p) = \begin{cases} 0 & \text{for } p = 1, \\ \frac{p+1}{3p} - \frac{1}{2p} = \frac{2p-1}{6p} & \text{for } p \geqslant 2. \end{cases} \quad (5)$$

For the M-type chain, both edges have zero probability of activation. Therefore, $A_M(p)$ can be calculated as

$$A_M(p) = \begin{cases} 0 & \text{for } p \leqslant 2, \\ \frac{p+1}{3p} - 2 \cdot \frac{1}{2p} = \frac{p-2}{3p} & \text{for } p \geqslant 3. \end{cases} \quad (6)$$

3.2.3. Number of chains generated from each type of idle chains

We now calculate the number of chains that are generated from each type of chain. There are five cases of chain generation, which are I to E, I to M, E to E, E to M, and M to M. We define a function $N_{xy}(q|p)$ as the expected number of y-type chains with length q generated from x-type chain with length p where $x,y \in \{I,E,M\}$. The detailed analysis to obtain $N_{xy}(q|p)$ is presented in the Appendix B.

For example, $N_{EM}(2|5)$ means the expected number of M-type chains with 2 idle FAPs generated after a contention from E-type chain with 5 idle FAPs. After contention, some of the idle FAPs can be activated and the chain may be divided into other types of chains. For instance, if the A_{I1} and A_{I3} are activated, the chain is divided into two M-type chains: One is with A_{I2} and the other with A_{I4} and A_{I5}. In this case, we have one M-type chain with 2 idle FAPs.

We validate the accuracy of the functions $N_{xy}(q|p)$. Fig. 9 shows that the result obtained from simulations coincides with the analytical result, where the symbols and lines represent the simulation and analytical results, respectively. In this comparison, we fix the length of the previous chain p at 8, and vary the generated chain length q from 1 to 8. The results confirm that our analysis is accurate.

3.2.4. Channel utilization

Let $S_m(j_1,\ldots,j_{r-1}|K)$ be a function that represents the number of chains during the rth contention round that has had j_1 idle FAPs after the first contention round, j_2 idle FAPs after the second contention round, and so on. K is the length of the initial chain. It is essential that a chain starts from type I and then changes its type to E or M. At any

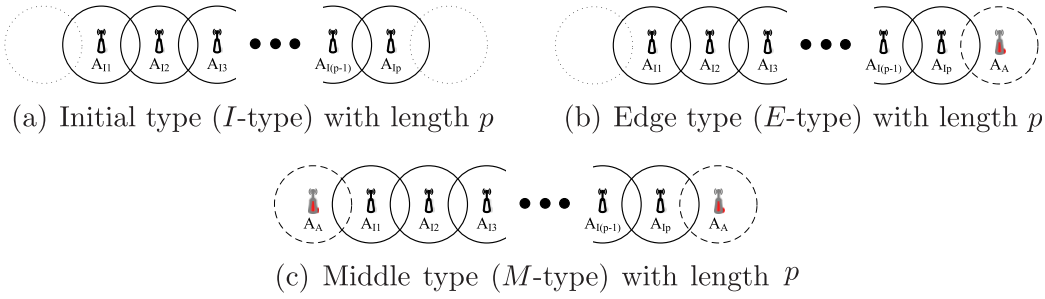

(a) Initial type (I-type) with length p (b) Edge type (E-type) with length p

(c) Middle type (M-type) with length p

Fig. 8. Types of inactive chains.

contention round, the chain can change to M if the type were E, but the change from M to E is impossible. Therefore, an important point is when the chain changes its type to M. Let the value m indicate this changing point. If $m = 1$, an M-type chain is formed after the first contention. If $m = r$ and r is the current round, the chain has no history of having been M-type. That is, it stays at E-type until the $(r-1)$th round. Therefore, using the $N_{xy}(q|p)$ function, we can obtain $S_m(\cdot)$ as

$$S_m(j_1,\ldots,j_{r-1}|K) = N_{x_1y_1}(j_1|K)N_{x_2y_2}(j_2|j_1)\cdots N_{x_{r-1}y_{r-1}}(j_{r-1}|j_{r-2}). \tag{7}$$

Here, (x_k,y_k) is selected according to m as

$$(x_k,y_k) = \begin{cases} \begin{cases} (I,M) & \text{for } k=1 \\ (M,M) & \text{for } 2 \leqslant k \leqslant r-1 \end{cases} & \text{for } m=1, \\ \begin{cases} (I,E) & \text{for } k=1 \\ (E,E) & \text{for } m \neq 2,\ 2 \leqslant k < m \\ (E,M) & \text{for } k=m \\ (M,M) & \text{for } m < k \leqslant r-1 \end{cases} & \text{for } m>1. \end{cases} \tag{8}$$

Let $\delta_r(K)$ be an increment of the channel utilization after the rth contention. For the first contention round, $\delta_1(K) = P_I(K)$. For $r \geqslant 2$, we can get $\delta_r(K)$ from (7). We have

$$\delta_r(K) = \begin{cases} A_I(K) & \text{for } r=1, \\ \sum_{j_1=1}^{K}\sum_{j_2=1}^{j_1}\cdots\sum_{j_{r-1}=1}^{j_{r-2}}\left(\sum_{m=1}^{r-1}A_M(j_{r-1})S_m(j_1,\ldots,j_{r-1}|K)\right. & \\ \left. +A_E(j_{r-1})S_r(j_1,\ldots,j_{r-1}|K)\right) & \text{for } r \geqslant 2. \end{cases} \tag{9}$$

Therefore, when the number of FAPs is K, the channel utilization after the contention of R-round, U_R, is given by

$$U_R = \sum_{r=1}^{R}\delta_r(K). \tag{10}$$

3.2.5. Analytical results and improvement rate

Fig. 10 shows the analytical results. We plot the FAP channel utilization, and the improvement rate of the channel utilization with the number of rounds. If the network does not use multi-frame contention mechanism, i.e. $R = 1$, the channel utilization is given as follows. For $K = 1$ and 2, the channel utilizations are 1 and 1/2, respectively. The channel utilization decreases with the number of FAPs, and from (3) it converges to one third as the number of FAPs goes to infinity.

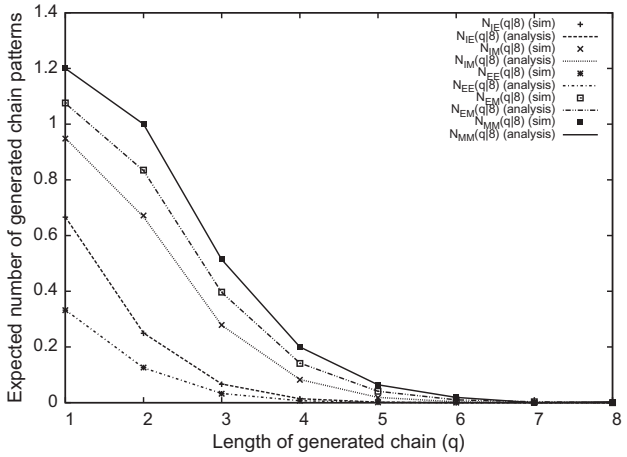

Fig. 9. Comparison between simulation and analysis results for $N_{xy}(q|p)$ when $p = 8$.

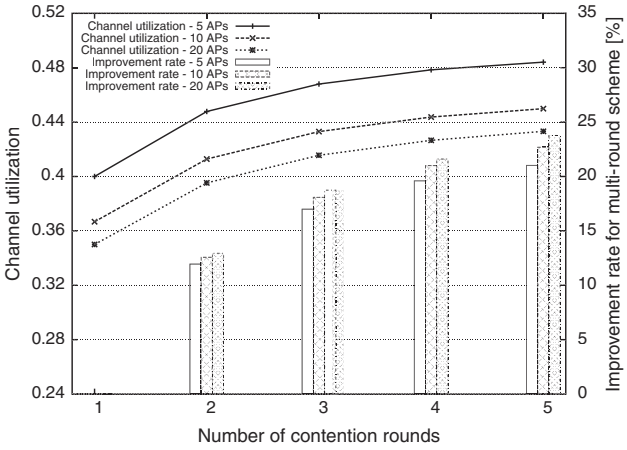

Fig. 10. FAP channel utilization and improvement rate using multi-frame contention.

However, our proposed multi-frame contention enhances the channel utilization. With the number of contention rounds R, more FAPs can be activated although the increase in the rate of improvement gradually decreases. If we increase R from 1 to 2, our scheme enables 10% more FAPs to be activated, while the improvement rate is over 20 percent if $R \geqslant 4$. However, the contention of fourth rounds shows an improvement rate increase of less than 5 percent when compared to that of the first three rounds. These

results suggest that three round contention is good enough for multi-frame contention for the chain topology.

4. Simulation results

In this section, we compare the performance of our FAP contention based scheduling scheme with that of a legacy non-contention based scheme in terms of capacity and fairness for a densely deployed femtocell network. We do not compare our proposed scheme with other frequency based femto-femto interference mitigation schemes because the frequency based solutions are orthogonal with ours. Our proposed scheme reduces the femto-femto interference installed in the same frequency. Instead, we compare our proposed scheme with a power adjustment based interference mitigation scheme in [7,8]. It is designed for each FAP to adjust its transmission power according to the interference level from neighboring cells. In densely deployed networks, this type of power control scheme, however, becomes the same as the legacy scheme with no contention in our simulation scenario, that is, all the FAPs use the same full power.

4.1. Simulation settings

Each FAP runs as a closed subscriber group, that is, an MN can only communicate with its associated FAP even though the signal strengths from some other FAPs are stronger. Our proposed scheme uses the multi-frame contention of $R = 3$. We consider a 10 by 10 grid topology as shown in Fig. 11. The distance between two neighboring FAPs and the transmission range of each FAP are set to 10 meters. Then various transmission ranges are tried in simulations under the same fixed distance. Each FAP has the same transmission range and the channels have the path loss exponent of 4. We do not consider short term fading. The maximum and minimum transmission powers of FAPs are -10 and -30 dBW, respectively, as given in [20]. The background noise is set to 94.5 dB. When the transmission range increases, the interference level also increases. MNs associated with an FAP are uniformly distributed within its transmission range. We also let the interference range be twice the transmission range. Within an interference area, each MN suffers from interference and cannot decode interferers' frames correctly.

4.2. Spectral efficiency

The Shannon capacity equation $C = \log_2(1 + SINR)$ is used to get the spectral efficiency, where SINR is calculated from the distance between MN and FAP. Fig. 12 shows the spectral efficiencies. The results show that our proposed scheme doubles the legacy capacity. To use our proposed scheme, the frame structure adds some additional overhead, i.e. AEC/AICs pairs. 15% and 30% of overhead indicates that 15% and 30%, respectively, of each frame are wasted for multi-frame contention, i.e. AEC/AICs pairs. Note that even with a 30% overhead, our proposed scheme outperforms the legacy scheme.

4.3. CDF of spectral efficiency

The cumulative distribution functions (cdf) of spectral efficiency for the transmission ranges of 10, 20, and 30 m are shown in Fig. 13. Our proposed scheme in the graphs is with the additional overhead of 15%. To cover the entire area, we uniformly place 200 MNs. Each MN probes the *SINR* and calculates its Shannon capacity.

Fig. 13(a) shows the cdf of spectral efficiency for the transmission range of 10 m. In this case, only a small number of MNs experience low throughput since the MNs experience relatively low interference. In our proposed scheme, there are few MNs that have throughput lower than 0.5 b/s/Hz while there are more than 40% such MNs in the legacy scheme.

In the case of 20-meter transmission range, the interference among MNs increases. As shown in Fig. 13(b), the fraction of the low capacity MNs increases. In the legacy scheme, almost 70% of the MNs cannot be served from their associated FAPs due to low SINRs. However, in our scheme, less than 10% of the MNs have capacity lower than

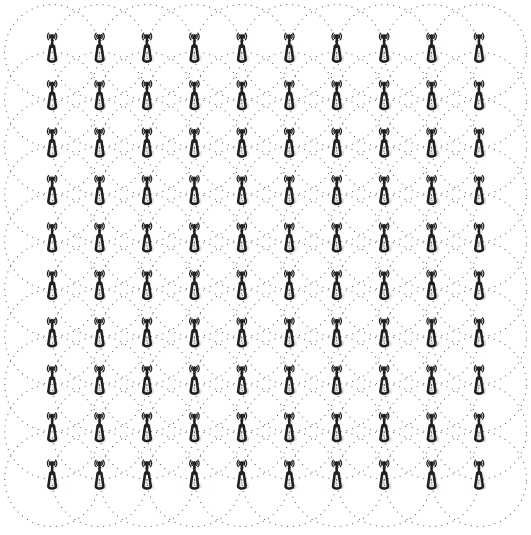

Fig. 11. Simulation topology of 10-by-10 FAP grid.

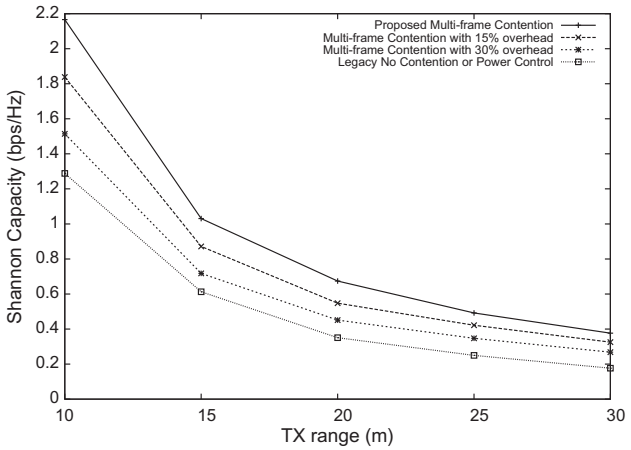

Fig. 12. Shannon capacity (spectral efficiency).

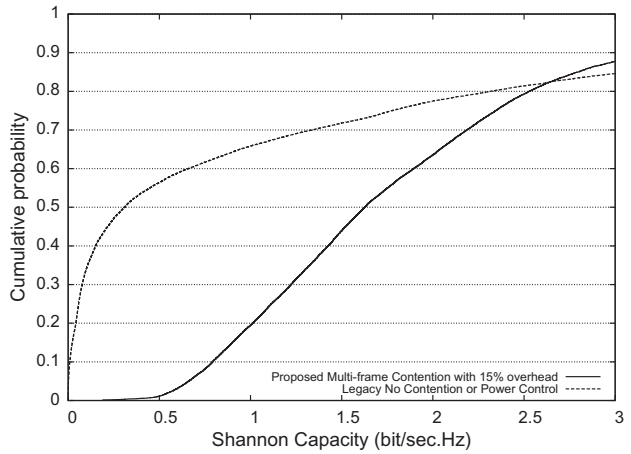

(a) Transmission range of 10m

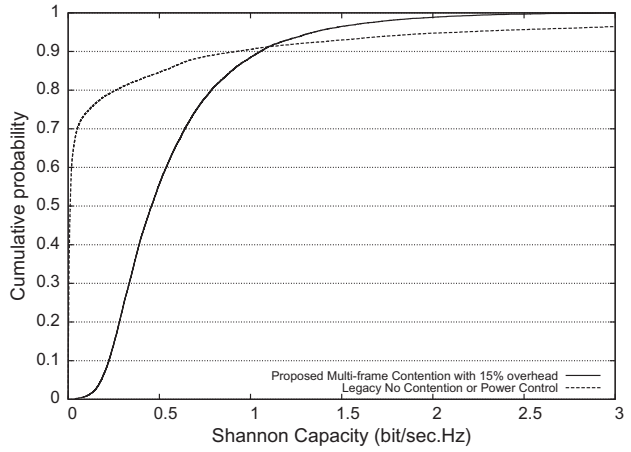

(b) Transmission range of 20m

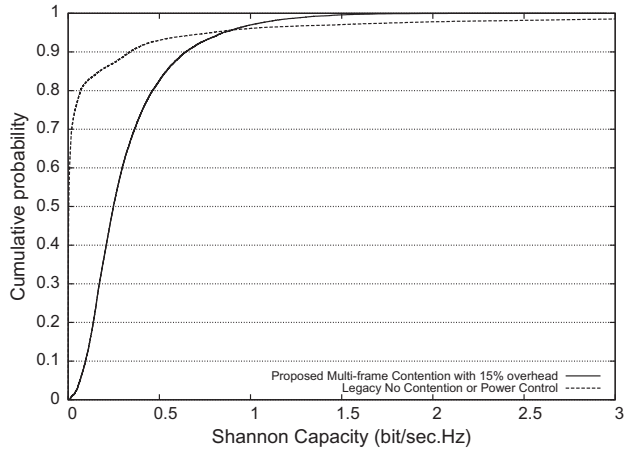

(c) Transmission range of 30m

Fig. 13. Cumulative distribution functions of the channel capacity.

0.25 b/s/Hz. From these results, we can infer that our proposed scheme considerably reduces the outage ratio.

Fig. 13(c) shows the cdf for the case of 30-meter transmission range. Since the distance between nearby FAPs is 10 m, an MN in the center of the topology may be interfered by approximately 25 neighboring FAPs. In spite of the severe interference, our proposed scheme still serves every MN with a lower capacity.

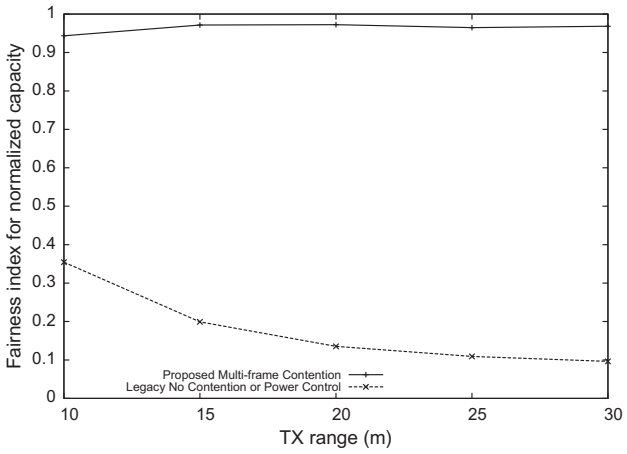

Fig. 14. Fairness index for capacity.

4.4. Fairness index

For fairness comparison, we use a normalized capacity of each MN. That is, each MN's capacity is normalized by the maximum capacity that can be achieved without interference. Then, we use the Jain's fairness index [21] for comparison. Thus, if there is no interference at all, the system has the maximum index of '1.'

As shown in Fig. 14, our proposed scheme achieves good fairness. Since the interference range is longer than the data transmission range, our proposed scheme cannot have the perfect fairness. In the legacy scheme, MNs at the cell edge area suffer from serious interference, so the capacity gap between cell edge and center users is significant.

5. Conclusion

As the market for home wireless networks grows, femtocell access points (FAPs) are expected to increase in popularity. However, for a city with a high population density, the interference from and among femtocells poses a serious challenge. In this paper, we proposed a novel frame structure for FAP contention based scheduling that aims to mitigate interference in a densely deployed wireless network. Our scheme runs in a fully distributed manner and chooses only one FAP out of interfering FAPs to be active for each time frame with the help of mobile devices, and allows the chosen FAP to exclusively use the next time frame. This scheme reduces the overall network interference, thereby achieving significantly higher channel efficiency. The simulation and analytical results reveal that our FAP contending scheme outperforms legacy non-contending scheme.

Since the current femtocell standard does not allow the modification of mobile devices, the interference problem is a very challenging one to solve. However, it is impossible to solve this problem without the help of the mobile devices since the main cause of interference comes from themselves. Accordingly, future standards should consider modifying mobile devices to mitigate the interference in some way. In such a case, the proposed FAP contention based scheduling scheme could be a promising candidate solution.

Acknowledgement

This research was partially supported by the KCC (Korea Communications Commission), Korea under the R& D program supervised by the KCA (Korea Communications Agency) (KCA-2011-08913-04003).

This work was partially supported by the National Research Foundation of Korea (NRF) Grant funded by the Korea government (MEST) (No. 2011-0027517).

Appendix A. Proof of Lemma 1

Proof. Let us denote the activation probability of A_i as P_i. Then, we calculate P_i as follows. For $K = 1$, the channel utilization is obviously one, so we focus on the case when $K \geqslant 2$.

1. For $i = 1$ (or K):
   Our tie breaking rule is to choose a winner randomly. Hence,

$$\begin{aligned} P_i &= \Pr\{r_1 < r_2\} + \Pr\{A_1 \text{wins} | r_1 = r_2\}\Pr\{r_1 = r_2\} \\ &= \Pr\{r_1 < r_2\} + \frac{1}{2}\Pr\{r_1 = r_2\} \\ &= \sum_{j=0}^{W-1} \Pr\{r_1 = j\}\Pr\{r_2 > j\} \\ &\quad + \frac{1}{2}\sum_{j=0}^{W-1} \Pr\{r_1 = j\}\Pr\{r_2 = j\} \\ &= \sum_{j=0}^{W-1}\left(\frac{1}{W}\cdot\frac{W-1-j}{W}\right) + \frac{1}{2}\sum_{j=0}^{W-1}\left(\frac{1}{W}\cdot\frac{1}{W}\right) \\ &= \frac{W-1}{2W} + \frac{1}{2W} = \frac{1}{2}. \end{aligned} \tag{A.1}$$

2. For $1 < i < K$:
   We now have four tie breaking cases. For each case, we obtain the following.

$$\begin{cases} \Pr\{r_i < r_{i-1}, r_i \leqslant r_{i+1}\} = \frac{1}{W}\sum_{j=0}^{W-1}\left(\frac{W-1-j}{W}\cdot\frac{W-j}{W}\right) = \frac{(W-1)(W+1)}{3W^2}, \\ \Pr\{r_i < r_{i-1}, r_i < r_{i+1}\} = \frac{1}{W}\sum_{j=0}^{W-1}\left(\frac{W-1-j}{W}\right)^2 = \frac{(W-1)(2W-1)}{6W^2}, \\ \Pr\{r_i \leqslant r_{i-1}, r_i \leqslant r_{i+1}\} = \frac{1}{W}\sum_{j=0}^{W-1}\left(\frac{W-j}{W}\right)^2 = \frac{(W+1)(2W+1)}{6W^2}, \\ \Pr\{r_i \leqslant r_{i-1}, r_i < r_{i+1}\} = \frac{(W-1)(W+1)}{3W^2}. \end{cases} \tag{A.2}$$

Therefore, we have

$$\begin{aligned} P_i = \frac{1}{4}\Bigg(2\cdot\frac{(W-1)(W+1)}{3W^2} + \frac{(W-1)(2W-1)}{6W^2} \\ + \frac{(W+1)(2W+1)}{6W^2}\Bigg) = \frac{4W^2-1}{12W^2}. \end{aligned} \tag{A.3}$$

From (A.1) and (A.3), we can calculate the average channel utilization U as

$$\begin{aligned} U &= \frac{1}{K}\sum_{i=1}^{K} P_i = \frac{1}{K}\left(2\cdot\frac{1}{2} + (K-2)\cdot\frac{4W^2-1}{12W^2}\right) \\ &= \frac{K+1}{3K} - \frac{K-2}{12KW^2}. \qquad \square \end{aligned} \tag{A.4}$$

Appendix B. Calculation of $N_{IE}(q|p)$

This appendix presents the detailed calculation for $N_{IE}(q|p)$ and the other four functions, i.e. $N_{IM}(q|p)$, $N_{EE}(q|p)$, $N_{EM}(q|p)$, and $N_{MM}(q|p)$, are presented in [22] due to the limited space.

We define a function $P^y(i,q)$ that returns the probability of generating a y-type chain with length q whose first inactive FAP is A_{Ii} from Fig. 7. According to the definition, $N_{IE}(q|p)$ can be expressed as

$$N_{IE}(q|p) = \sum_{i=1}^{p-q+1} P^E(i,q). \tag{B.1}$$

For $p = 1$ and 2, we can intuitively obtain $N_{IE}(1|1) = 0$, $N_{IE}(1|2) = 1$, and $N_{IE}(2|2) = 0$. For $p \geqslant 3$, if $q = p$, we have $N_{IE}(q|p) = 0$, but if $q = p-1$, $N_{IE}(q|p) = P^E(1,p-1) + P^E(2,p-1)$. Obviously, $P^E(1,p-1)$ and $P^E(2,p-1)$ have the same probability, and we denote these as $\pi_1(p-1)$ in the following. Also, if $q \leqslant p-2$, $N_{IE}(q|p) = P^E(1,q) + P^E(p-q+1,q)$. Because of the symmetry, $P^E(1,q)$ and $P^E(p-q+1,q)$ have the same value, and we define these two functions as $\pi_2(q)$.

Then, we have

$$N_{IE}(q|p) = \begin{cases} 0 \quad \text{for } q = 1 & \text{for } p = 1, \\ \begin{cases} 1 & \text{for } q = 1 \\ 0 & \text{for } q = 2 \end{cases} & \text{for } p = 2, \\ \begin{cases} 0 & \text{for } q = p \\ 2\pi_1(q) & \text{for } q = p-1 \\ 2\pi_2(q) & \text{for } q \leqslant p-2 \end{cases} & \text{for } p \geqslant 3. \end{cases} \tag{B.2}$$

We now calculate $\pi_1(q)$ and $\pi_2(q)$. Assuming the infinite contention window size, i.e. ignoring the possibility of having the same random number, the only case to consider is the number of permutation cases. Though we are considering on the chain of q idle FAPs, we need to consider more than q FAPs to create the request pattern. Note that, the chain from A_{I1} to A_{Iq} is an idle chain that we want to create.

To generate the $\pi_1(q)$ pattern, we need to consider $(q+1)$ FAPs. As shown in Fig. B.15, all the FAPs have their own random contention numbers in descending order. Then, we have

$$\pi_1(q) = Pr\{r_{I1} < r_{I2} < \cdots < r_{Iq} < r_{I(q+1)}\} = \frac{1}{(q+1)!}. \tag{B.3}$$

In the pattern $\pi_2(q)$, $(q+2)$ FAPs are considered as shown in Fig. B.16. From r_{I1} to $r_{I(q+1)}$, each FAP must select a random contention number in descending order, but the last FAP $A_{I(q+2)}$ chooses a larger random number than $A_{I(q+1)}$ does, i.e. $r_{I(q+1)} < r_{I(q+2)}$. To create this pattern, we first pick one number from the random number pool except the minimum and set it to $r_{I(q+2)}$, then allocate the remaining numbers in descending order. Therefore, we have

$$\pi_2(q) = \frac{1}{(q+2)!}\binom{q+1}{1} = \frac{q+1}{(q+2)!}. \tag{B.4}$$

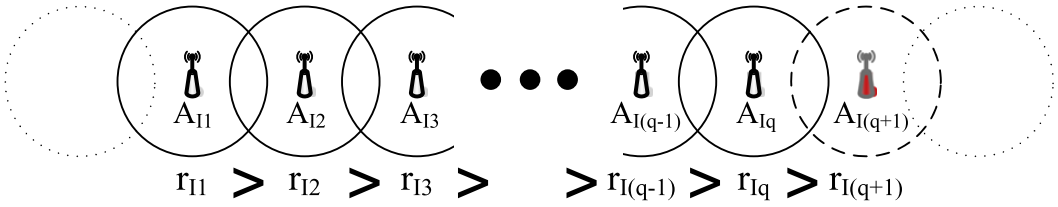

Fig. 15. Pattern for $\pi_1(q)$.

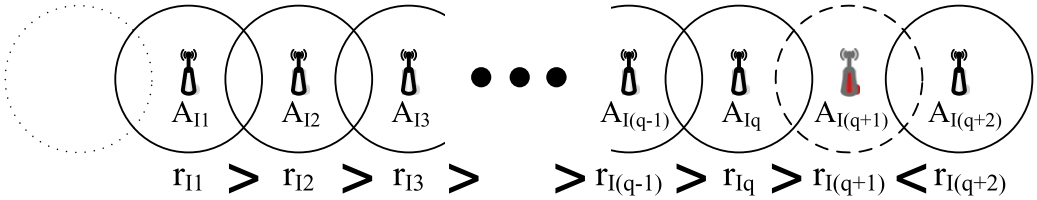

Fig. 16. Pattern for $\pi_2(q)$.

References

[1] M.-S. Alouini, A.J. Goldsmith, Area spectral efficiency of cellular mobile radio systems, IEEE Trans. Veh. Tech. 48 (4) (1999) 1047–1066.

[2] A. Damnjanovic, J. Montojo, Y. Wei, T. Ji, T. Luo, M. Vajapeyam, T. Yoo, O. Song, D. Malladi, A survey on 3GPP heterogeneous networks, IEEE Wireless Commun. 18 (3) (2011) 10–21.

[3] V. Chandrasekhar, J.G. Andrews, Femtocell networks: a survey, IEEE Commun. Mag. 46 (9) (2008) 59–67.

[4] <http://www.anygate.co.kr/product.php?prod=etc_wireless>.

[5] O. Simeone, E. Erkip, S. Shamai, Robust transmission and interference management for femtocells with unreliable network access, IEEE J. Sel. Areas Commun. 28 (9) (2010) 1469–1478.

[6] J. Lim, D. Hong, Management of neighbor cell lists and physical cell identifiers in self-organizing heterogeneous networks, J. Commun. Netw. 13 (4) (2011) 367–376.

[7] M.-S. Kim, H.W. Je, F.A. Tobagi, Cross-tier interference mitigation for two-tier OFDMA femtocell networks with limited macrocell information, in: Proceedings of IEEE GLOBECOM, Miami, USA, December 2010.

[8] H.-S. Jo, C. Mun, J. Moon, J.-G. Yook, Self-optimized coverage coordination in femtocell networks, IEEE Trans. Wireless Commun. 9 (10) (2010) 2977–2982.

[9] O. Bulakci, S. Redana, B. Raaf, J. Hamalainen, Impact of power control optimization on the system performance of relay based LTE-advanced heterogeneous networks, J. Commun. Netw. 13 (4) (2011) 345–359.

[10] C.-H. Ko, H.-Y. Wei, On-demand resource-sharing mechanism design in two-tier OFDMA femtocell networks, IEEE Trans. Veh. Tech. 60 (3) (2011) 1059–1071.

[11] Y. Shi, A.B. Mackenzie, L.A. Dasilva, K. Ghaboosi, M. Latva-Aho, On resource reuse for cellular networks with Femto- and Macrocell coexistence, in: Proceedings of IEEE GLOBECOM, Miami, USA, December 2010.

[12] Y.-Y. Li, M. Macuha, E.S. Sousa, T. Sato, M. Nanri, "Cognitive Interference Management in 3G Femtocells," in Proceedings of IEEE PIMRC, Tokyo, Japan, September 2009.

[13] K. Sundaresan and S. Rangarajan, "Efficient Resource Management in OFDMA Femto Cells," in Proceedings of ACM MobiHoc, Louisiana, USA, May 2009.

[14] M.Y. Arslan, J. Yoon, K. Sundaresan, S.V. Krishnamurthy, S. Banerjee, "FERMI: A femtocell resource management system for interference mitigation in OFDMA networks," in: Proceedings of ACM MobiCom, Las Vegas, USA, September 2011.

[15] R1-101505, "Extending Rel-8/9 ICIC into Rel-10," Qualcomm incorporated, February 2010.

[16] 3GPP TR 36.300, "E-UTRA and E-UTRAN; Further Overall description."

[17] L.G.U. Garcia, G.W.O. Costa, A.F. Cattoni, K.I. Pedersen, P.E. Mogensen, Self-organizing Coalitions for Conflict Evaluation and Resolution in Femtocells, in: Proceedings of IEEE GLOBECOM, Miami, USA, December 2010.

[18] F. Pantisano, M. Bennis, W. Saad, R. Verdone, M. Latva-aho, Coalition formation games for femtocell interference management: a recursive core approach, in: Proceedings of IEEE WCNC, Quintana-Roo, Mexico, March 2011.

[19] IEEE Std 802.16-2009, IEEE Standard for Local and Metropolitan Area Networks Part 16: Air Interface for Fixed and Mobile Broadband Wireless Access Systems, IEEE Press, May 2009.

[20] Femto forum, "Interference Management in OFDMA Femtocells," March 2010, pp. 109–110.

[21] R. Jain, D. Chiu, and W. Hawe, "A Quantitative Measure of Fairness and Discrimination for Resource Allocation in Shared Systems," Technical Report, DEC TR-301, Littleton, USA, 1984.

[22] J. Yun, Contention Based Distributed Access Control for Wireless Networks, Ph.D. Thesis, Seoul National University, 2008.

Jeongkyun Yun received the B.S., M.S., and Ph.D. degrees from School of Electrical Engineering and Computer Science, Seoul National University, Seoul, Korea, in 2001, 2003, and 2008, respectively. He is currently working in LG Electronics as a senior research engineer. His research interests include future wireless LAN protocols, next generation cellular networks, and ad hoc networks.

Sung-Guk Yoon is currently a Ph.D. candidate in the School of Electrical Engineering and Computer Science, Seoul National University. He received his B.S. degree from Seoul National University, in 2006. His research interests include next generation cellular networks, cross-layer optimization, resource management, and power line communications.

Jin-Ghoo Choi received the B.S., M.S., and Ph.D. degrees in the school of Electrical Engineering & Computer Science, Seoul National University in 1998, 2000, and 2005, respectively. From 2006 to 2007, he worked for Samsung Electronics as a senior engineer. In 2009, he was with the Department of Electrical & Computer Engineering in The Ohio State University as a visiting scholar. He joined the Department of Information and Communication Engineering in Yeungnam University as a faculty member in 2010. His research interests include performance analysis of communication networks, packet scheduling policy in wireless networks, and wireless sensor network.

Saewoong Bahk received B.S. and M.S. degrees in Electrical Engineering from Seoul National University in 1984 and 1986, respectively, and the Ph.D. degree from the University of Pennsylvania in 1991. From 1991 through 1994 he was with AT& T Bell Laboratories as a member of technical staff where he worked for AT& T network management. In 1994, he joined the school of electrical engineering at Seoul National University and currently serves as a professor. He has been serving as TPC members for various conferences including ICC, GLOBECOM, INFOCOM, PIMRC, WCNC, etc. He is on the editorial board of Journal of Communications and Networks (JCN). His areas of interests include performance analysis of communication networks and network security. He is an IEEE senior member and a member of Who's Who Professional in Science and Engineering.